Journal of the Chinese Society of Mechanical Engineers, Vol.47, No.1, pp17~25 (2026)

Trajectory Planning Based Precise Positioning Control of an X-Y Platform

Haris Khan*, Hsiu-Ming Wu **and Chung-Wei Chen *

Keywords : X-Y platform, Trajectory planning, Trapezoidal velocity profile, Decentralized PID controllers.

ABSTRACT

The study aims to attain precise positioning control of an X-Y platform. Here, square and circular motion trajectories with a trapezoidal velocity profile are planned. Subsequently, decentralized PID controllers are designed to track the predefined reference trajectories. The corresponding experiments are conducted to validate the effectiveness and feasibility of the proposed control scheme. In terms of the experimental results, the average positioning error is smaller than 0.0164 mm in the square trajectory and 0.02265 mm for the circular trajectory. It is evident that the system demonstrates satisfactory control performance despite suffering the saturation effect or a sudden disturbance.

INTRODUCTION

With the rapid growth of the high-end equipments in the manufacturing industry and the demand for precision products (Wu et al. 2020), the CNC machine has a wide range of applications to keep down production time and cost in the fabricating fields. Consider that CNC machines often performs high-precision motion and works at its limits (Kung, Anh and Jou 2008), such as laser cutting and component machining (Wang, He and Cao 2021; Hu et al. 2011), the stability and precision may be worsen while suffering excessive long-term vibrations (Chang, Hsia and Huang 2018). Therefore, this issue for the challenging of precision positioning has been studied by experts who have proposed a variety of schemes, usually zooming in on the design and implementation of control laws (Nguyen, Saussie and Saydy 2021; Guo et al. 2019), or the proposal of reference motion profiles (Tan et al. 2019).

As ones know, the development of control laws has been exhaustively studied, however, the motion profile planning is also a key topic to diminish the vibration effects by manipulating system dynamics through the profile definition. Typically, the movement trajectories are the set of points arranged into various curves to ensure that the system complies with its own dynamic conditions (Guo et al. 2019), such as maximum velocity and maximum voltage. In this sense, there has been exploring methods to generate motion patterns to meet the constraint conditions. Krikelis and Barkas. (1984) designed an integrator combining a signal limiter to overcome actuator saturation. Other research has focused on avoiding voltage saturation by reconstructing the PI voltage controller in vector-controlled induction motors (Ohishi and Mashimo, 1997; Ohishi et al., 2006). Considering the dynamics profile of control system, Huang et al. (2022) use the most common movement scheme (i.e., the trapezoidal velocity motion profile) which is planned acceleration/ deceleration time achieved by the motion controller making periodic reciprocating motions within the specified time. The above method will lead to sudden acceleration variation that includes a high jerk. In current approaches, the method is used to alleviate the trapezoidal motion profile effect known as the S curve profile (Biagiotti and Melchiorri 2021). A smooth jerk pattern is obtained by 3rd-degree polynomial equation, and there are also higher-order equations studied in (Masoudi, Feyzi and Sharifian 2016; Wang et al. 2018). The smooth jerk profile brings physical and mechanical benefits to motors. Despite having some drawbacks, the trapezoidal profile is still widely used in industries due to its ability to complete tasks within a specified time range with superior efficiency. Other velocity patterns may have a disadvantage in extending total execution time to ensure jerk smoothness by large amounts of computation (Yoon et al. 2019). On the contrary, the trapezoidal profile yields a rapid implementation with less complex calculations in commercial industrial robots.

Paper Received December, 2024. Revised April, 2024. Accepted April, 2024. Author for Correspondence: Hsiu-Ming Wu.

* *Graduate Student, Institute of Mechatronic Engineering, National Taipei University of Technology, Taipei, Taiwan 10608, ROC.*

** *Associate Professor, Department of Intelligent Automation Engineering, National Taipei University of Technology, Taipei, Taiwan 10608, ROC.*

This work focuses on the motion profile planning, in which predefined trajectories satisfy the machine dynamics and offer smoothness in system motion during execution while mitigating the error effects caused by input saturation. As a result, this study achieves the fast response time can be achieved with an underdamped response. This control scheme is implemented on the X-Y platform, which combines two servo motors and the ball screw proved the feasibility of the proposed methodology.

The rest of the paper is arranged as follows: the architecture of the X-Y platform and the problem statement are introduced in Section II. Section Ⅲ describes the velocity profile for motion trajectories. In Section Ⅳ, design of decentralized PID controllers with each motor for motion control are addressed. Section Ⅴ presents and analyzes the experimental results and the conclusion is made in Section Ⅵ.

SYSTEM DESCRIPTION OF THE X-Y PLATFORM AND PROBLEM STATEMENT

In order to practically achieve precise positioning control with the proposed velocity profile, two servo motors serve as the driving mechanism in the X-Y platform. For the X-Y platform, an inner loop velocity control as shown in Fig. 1 is implemented by TECO Inc. drivers. The resolution of the linear encoder is 0.5 um. To minimize the deviation between reference and actual positions, the design of the motion controller is an important part in this approach, and the proposed method will be discussed later. The top view of the experimental setup is shown in Fig. 2 and Table 1 is the specification for motors. Since the designed motion controller is implemented on a PC, external device connections are required to control and read information from the motors. Figure 3 depicts the framework of the X-Y control system platform.

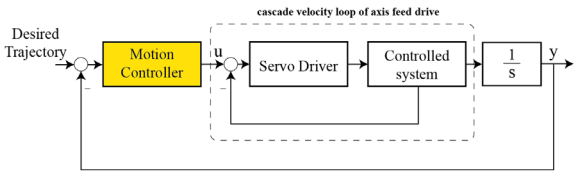

Figure 1. Overall control block of the X-Y platform system.

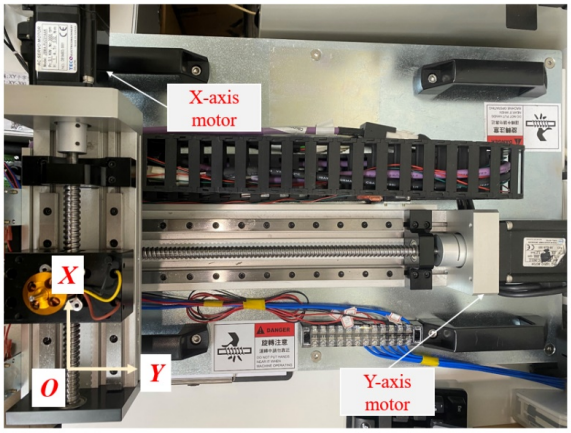

Figure 2. X-Y platform used in the experiment.

As shown in Fig. 3, the X-Y platform is configured with two external devices: a digital-to-analog (PCI-1716) converter and a pulse counter for real-time (PCI-1200U) positioning control design. The communicate protocol Real-Time Workshop (RTW) is taken charge of each equipment connected. The above architecture is constructed a precise position tracking control for the position loop. The following sections will introduce the corresponding equipment used in this experiment.

Table 1. Specifications of the used driving motors

	X axis motor value	Y axis motor value
Rated power (kw)	0.1	0.4
Rated torque (Nm)	0.32	1.27
Rated current (A)	0.9	2.6
Base speed (rpm)	3000	3000
Rotor inertia (J)	0.041	0.28
Torgue constant (Kt)	0.36	0.47
Winding resistance (Ra)	25.4	3.15
Winding inductive (mH)	26.5	11

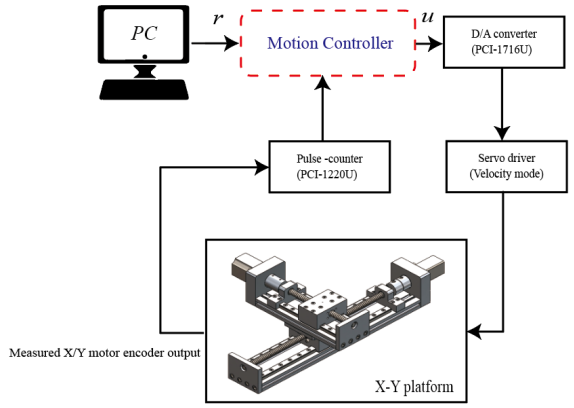

Figure 3. Hardware configuration of the X-Y control system platform.

A. Real-time workshop

The RTW is a module in Simulink, which enables communication with the D/A converter and pulse-count converter through a PC as shown in Fig. 3. RTW can generate optimized, portable, and modifiable C/C++ code from file format (e.g., .slx and .mdl) for model validation or prototype testing . The designed algorithm can communicate with the devices that connected to control system in real-time environments through RTW's real time function.

B. D/A converter

There are well know that the D/A converter is the device to convert digital data into an analog signal, and it is commonly utilized in robotic systems and digital circuits in industry scenario. Its primary function is taking binary digital input and produces a corresponding continuous analog output to plant. In this experiment, the PCI-1716 multifunction card is employed as the D/A converter for the purposed control system and the performance of PCI protocol can meet the requirements for real-time control.

C. Pulse-counter

A Pulse-counter is a device that converts the pulse signals generated by rotary or linear encoders into digital quantities, enabling measure the movement of position, velocity, and acceleration for motion control. In this experiment, The PCI-1200U multifunction card is utilized as a pulse-counter and it can efficiently and rapid transmit position data to the controller, achieving real-time control of the X-Y platform.

D. Problem statement

This study employs a velocity profile for trajectory planning, which can generate proper trajectories that satisfy physical conditions. Through this method, trajectories of different contours can be generated for motion of controlled systems. To ensure a stable system response for pre-defined trajectory, a motion controller is designed first. Then, a velocity profile planning is used to be incorporated into different cases. Finally, the planned trajectories are experimented with the X-Y platform, with the control objective being that the proposed decentralized PID controllers are designed and the suitable velocity profile planning is selected to achieve high-precision trajectory tracking results.

MOTION TRAJECTORY PLANNING

The trapezoidal velocity profile, also known as the T-velocity profile, is extensively studied in research (Jindal and Ragavan 2018; Heo et al. 2019) as it enables industrial motors to achieve periodic reciprocating motions and fast response. Figure 4 illustrates the shape and properties of a symmetric T-velocity profile. Before describing the velocity profile, some parameters such as maximum acceleration, maximum velocity, final point, and the end time should be predefined. The corresponding position $x(t)$, velocity $\dot{x}(t)$, and acceleration $\ddot{x}(t)$ are represented as follows:

$$x(t)=\begin{cases}\frac{1}{2}a_{\max}t^2 & 0\le t<t_1\\ \frac{1}{2}v_{\max}(2t-t_1) & t_1\le t<t_2\\ x_f-\frac{1}{2}a_{\max}(t_f-t)^2 & t_2\le t\le t_f\end{cases} \tag{1}$$

$$\dot{x}(t)=\begin{cases}\frac{v_{\max}}{t_1}t & 0\le t\le t_1\\ v_{\max} & t_1\le t<t_2\\ \frac{v_{\max}}{t_1}(t-t_f) & t_2\le t\le t_f\end{cases} \tag{2}$$

$$\ddot{x}(t)=\begin{cases}a_{\max} & 0\le t\le t_1\\ 0 & t_1\le t<t_2\\ -a_{\max} & t_2\le t\le t_f\end{cases} \tag{3}$$

where

$$v_{\max}=\frac{x_f}{t_2} \tag{4}$$

$$a_{\max}=\frac{x_f}{t_1t_2} \tag{5}$$

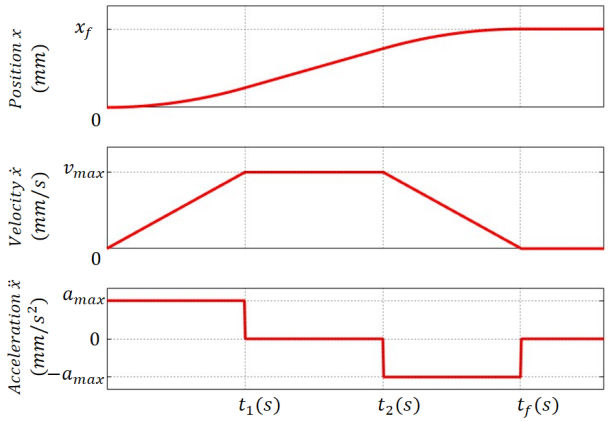

Figure 4. The trapezoidal velocity motion profile.

where x_f denotes target distance and t_f is end time. Basically, the trapezoidal velocity profile is divided the operation into three segments for execution through acceleration end time t_1 and deceleration start time t_2. To generate a workable motion profile, the above parameters need to satisfy constraints. Firstly, $a_{\max}$ and $v_{\max}$ parameters derived from the motion profile must be adjusted to be within their physical limits. The constraints for $a_{\max}$ and $v_{\max}$ are given by

$$\begin{cases} 0 \le v_{\max} = \dfrac{x_f}{t_2} \le v_{\lim} \\ 0 \le a_{\max} = \dfrac{x_f}{t_1 t_2} \le a_{\lim} \end{cases} \tag{6}$$

where $v_{\lim}$ and $a_{\lim}$ respectively represent the velocity and acceleration limits. Next, the acceleration and deceleration intervals of the trapezoidal velocity profile are usually designed to be symmetric. Hence, the total interval is presented related with the acceleration and deceleration time intervals as

$$t_f = t_1 + t_2 \tag{7}$$

By setting the constraint, a trapezoidal velocity profile is generated by setting the end time t_f and target distance x_f ensuring that the system can complete the motion trajectory task fastly and smoothly despite imposing loads on the mechanical components.

Next, we construct the second reference trajectory through arc interpolation. Due to the geometric properties of a circular path, the number of interpolation points needs to be firstly determined for executing the motion. Since the system motion is composed of straight line segments, the number of interpolation points determines the smoothness of the circular path in practical situations. The more the interpolation points are, the more smooth the system motion is. Then, the motion trajectory equation of the circular path is designed as

$$(x-h)^2 + (y-k)^2 = r^2 \tag{8}$$

where (h,k) represents the center coordinates of the circle; (x,y) stands for the coordinate points of the circular path, and r denotes the radius of the circle. After determination of the circular parameters using the above equations, circular motion trajectory points are generated and updated as a next control command represented in the following equations:

$$x_i = x_{i-1} + \Delta x \tag{9}$$

$$y_i = y_{i-1} + \Delta y \tag{10}$$

where x_i and y_i are the updated coordinates of the circular path, x_{i-1} and y_{i-1} are the coordinates of the previous iteration, Δx and Δy are the coordinate variation and i represents the updating number in the circular path. Consequently, the displacement of two adjacent coordinate points can be represented as

$$\Delta P = \sqrt{(x_i - x_{i-1})^2 + (y_i - y_{i-1})^2} \tag{11}$$

where $P_i = (x_i, y_i)$ represents the coordinate points on the circular path, and ΔP represents the coordinate increments for each segment. The magnitude of these ΔP values represents the roughness of the circular trajectory. The more increments mean the smoother of the circular trajectory that can be obtained. Figure 5 illustrates the circular interpolation process. Finally, the motion velocity along the circular trajectory depends on the ratio of ΔP to the execution time of ΔP. Because we know total sample point T_{sp} and time interval Δt is also known. Therefore, total execution time is equal to $T_{sp} \times \Delta t$ and total sample point is given by

$$T_{sp} = \frac{2\pi r}{\Delta P} \tag{12}$$

Hence, the motion velocity along the circular trajectory V_{arc} can be derived from the following relationship

$$V_{arc} = \frac{\Delta P}{\Delta t} \tag{13}$$

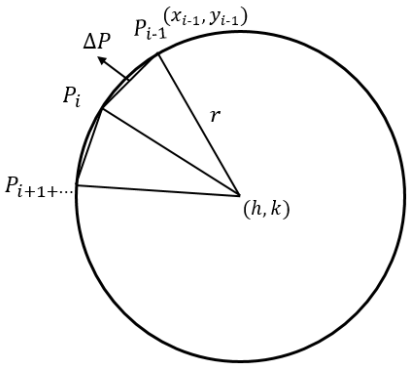

Figure 5. The circular interpolation representation diagram.

DECENTRALIZED PID TRAJECTORY -TRACKING CONTROLLER DESIGN

In this section, to ensure that the X-Y platform following the planned reference trajectory, the controller $\mathbf{u} = \begin{bmatrix} u_x & u_y \end{bmatrix}^T \in \Re^2$ is designed to achieve the control objective. As ones know, PID controllers possess characteristics of simple structure, easy implementation and high reliability. As a result, we here choose decentralized PID controllers as the control core. The theoretical expression for the PID controller is as follows:

$$\begin{cases} u_x = k_{Px} e_x + k_{Ix} \int_0^t e_x dt + k_{Dx} \dfrac{de_x}{dt} \\ u_y = k_{Py} e_y + k_{Iy} \int_0^t e_y dt + k_{Dy} \dfrac{de_y}{dt} \end{cases} \tag{14}$$

where k_{Px} and k_{Py} are the proportional gains; k_{Ix} and k_{Iy} denote the integral gains; k_{Dx} and k_{Dy} stand for the derivative gains; e_x and e_y are the position errors; u_x and u_y are the input voltages. By finding the appropriate proportional, integral, and derivative gains for both axes, the position errors are fast converged towards zero, namely, the control precision is enhanced.

EXPERIMENTAL VALIDATION AND RESULT DISCUSSIONS

To validate the performance of the designed motion controller (i.e., the decentralized PID controllers), two types of motion trajectories for the X-Y platform are investigated in this experiment. For the X-Y platform, the maximum span distance is 110 mm along the x-axis and 325 mm along the y-axis. In order to complete the precision trajectory tracking control, corresponding control gains have to be appropriately selected to avoid system instability or worse performance. Various approaches have been proposed to tune PID gains including the Ziegler-Nichols method and others (Masuda 2015; Liu et al. 2015) In the experiment, these control gains $k_{Px} = 3e-3$; $k_{Py} = 2e-4$; $k_{Ix} = 5e-5$; $k_{Iy} = 1e-5$; $k_{Dx} = 4e-4$; $k_{Dy} = 1e-6$ are used. In the beginning, a step reference change is tested. Physical limits for actuators are also investigated here. In general, input saturation may lead to system instability or degraded performance. Here, actuator saturation limits are set to 4.5 volts on the x-axis and 6 volts on the y-axis, and the relationship between saturation and the control system is explored. Figures 6 show the control system experiment with magnified transient response to a step reference change. It can be seen that system output fast tracks the reference in seconds without underdamping or overshooting. Apparently, the experimental results show that even within these saturation limits, the system still maintains satisfactory performance and demonstrates that the proposed controller has capabilities to deal with the system subjected to input saturations.

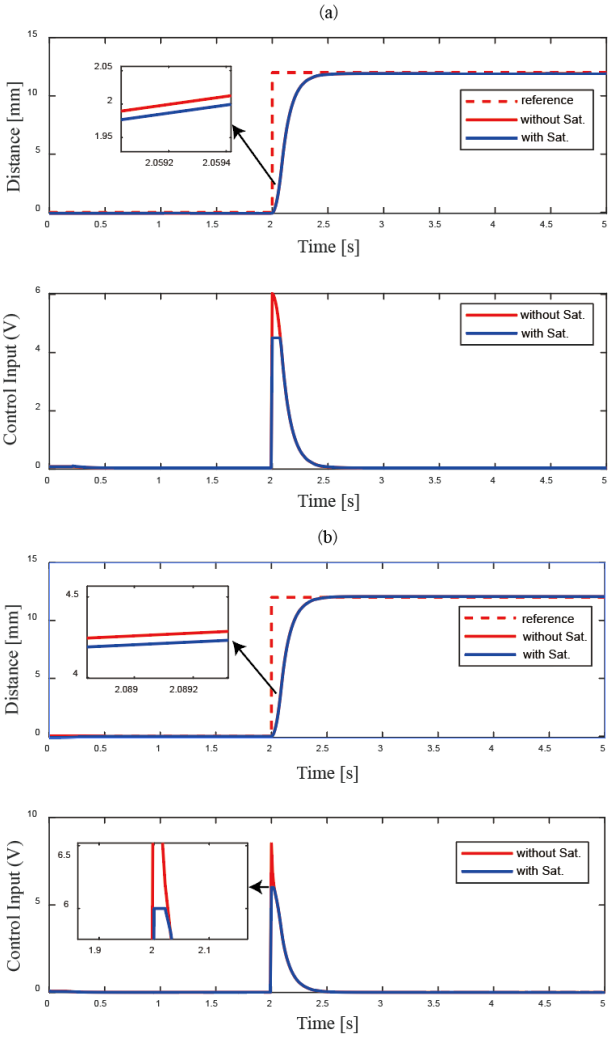

Figure. 6. Comparison of step responses under with and without input saturation on (a) x-axis and (b)

y-axis.

Then, the square path with the trapezoidal velocity profile is planned. The side length of the square reference trajectory is 40 mm, thus the final point x_f is set as 40 mm for each side of the trajectory. The parameters in Eqs. (1)~(3) are chosen as t_f = 3 seconds, v_{max} = 0.2 mm/s, and a_{max} = 0.2 mm/s^2 for each square trajectory motion. Note that the v_{max} must be under 13.3 mm/s; if the v_{max} exceeds 13.3 mm/s, the trapezoidal velocity profile will degenerate into a triangular profile without a constant velocity segment. The tracking response is shown in Fig. 7 From the responses, it can be clearly seen that the proposed PID controllers possess excellent control performance. Figure 8 shows the trajectory-tracking response of each axis in the X-Y platform. It can be seen that the motion of each axis can fast converge to the planned trajectory points and attains a high-precision positioning control. Through the trapezoidal velocity profile planning, the steady-state performance has to be ensured by minimize overshoot. It can reach the trajectory points in the specified time and satisfy the physics constraints by selecting design parameters (i.e., system's v_{max} and a_{max}). The corresponding velocity responses are shown in Fig. 9 where the T-velocity curve can be attained by differentiating the data obtained from the pulse counter, and Fig. 10 shows the tracking error of each axis. The steady-state errors of 0.0212 mm in the x-axis and 0.0116 mm in the y-axis demonstrate the minimum significant deviations achieved with the proposed controllers. The corresponding responses of the control inputs are given in Fig. 11.

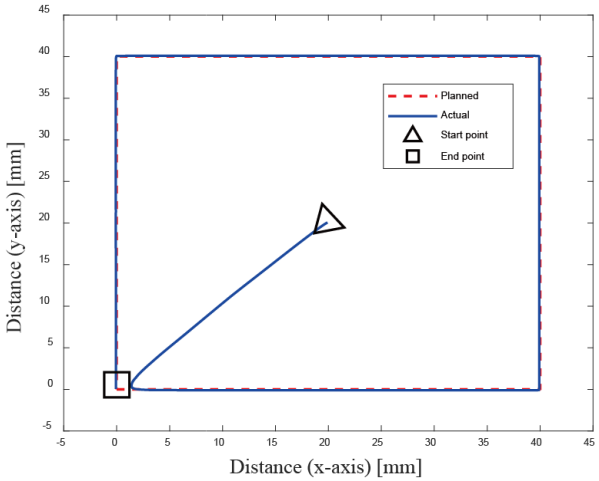

Figure 7. The tracking response of the square trajectory.

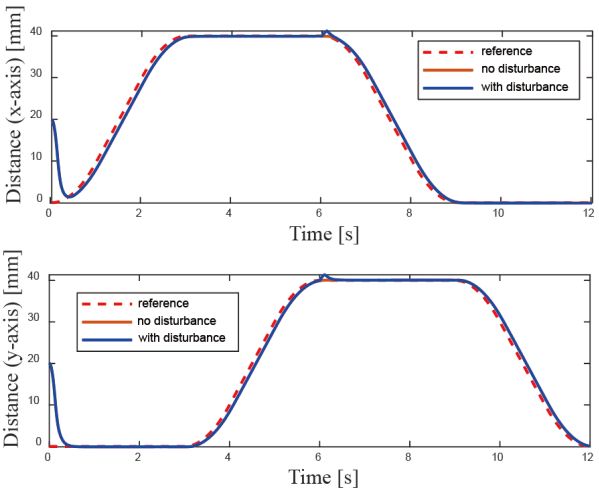

Figure 8. Responses of the square trajectory tracking in the x-axis and y-axis.

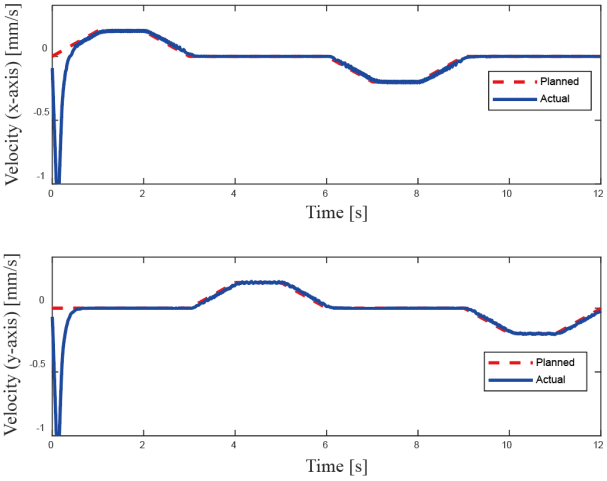

Figure 9. The velocity response of the square trajectory.

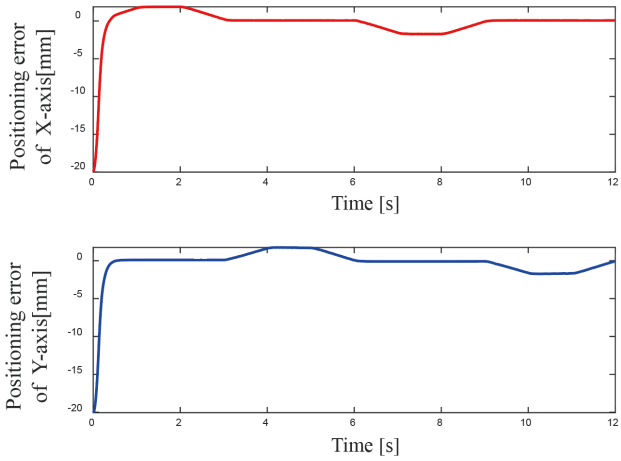

Figure 10. Responses of the square trajectory tracking errors in x and y-axes.

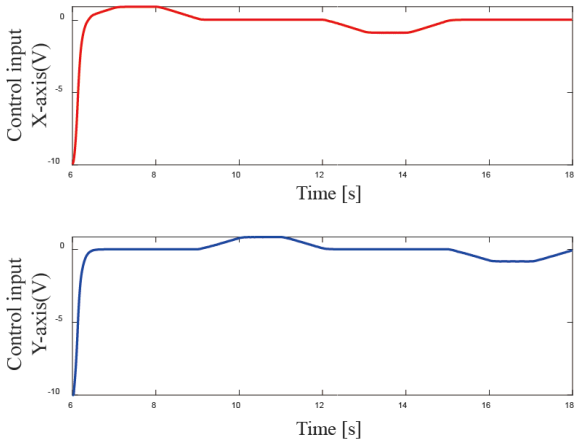

Figure 11. The control signal based on decentralized PID with square trajectory.

Subsequently, the circular trajectory is planned for the X-Y platform to verify the feasibility of the proposed control scheme. The corresponding parameters are set for this circular trajectory: center (0, 0), the radius of the circle r is set as 8 mm, the velocity can be obtained from Eq. (12) as 2.1 mm/s and the total sample points are 1200.

With the above settings, continuous path points can be obtained. The tracking response of the planned circular trajectory in the experiment is shown in Fig. 12 where the circular trajectory tracking responses of each axis are respectively exhibited in Figs. 12 and 13. It can be observed that the steady-state error is 0.032 mm on the x-axis and 0.014 mm for the y-axis in Fig. 14. It reveals that the proposed control scheme indeed can make the tracking errors converge to a bounded set. Fig. 15 shows the responses of the corresponding control inputs. Besides, to examine the system robustness, the external disturbance with 1 volt at 6 seconds is added in the square and circular paths. The corresponding responses are demonstrated in Figs. 16-19. It can be seen that the stabilized time is approximately 0.28 and 0.41 seconds after addition of the disturbance, respectively. The X-Y platform undergoes overshoots with oscillations that rapidly converge to the trajectory. However, if larger significant disturbances are added to the control system, the advanced control scheme (e.g., Active disturbance rejection control) could be discussed to address the complexity disturbance problem in the future. The experimental results demonstrate that the proposed control scheme still possesses a high level of robustness in dealing with sudden input disturbances. In summary, it turns out that the precise tracking control can be achieved and simultaneously meet the requirement of the planned T-curve velocity in spite of suffering input saturations or a sudden disturbance.

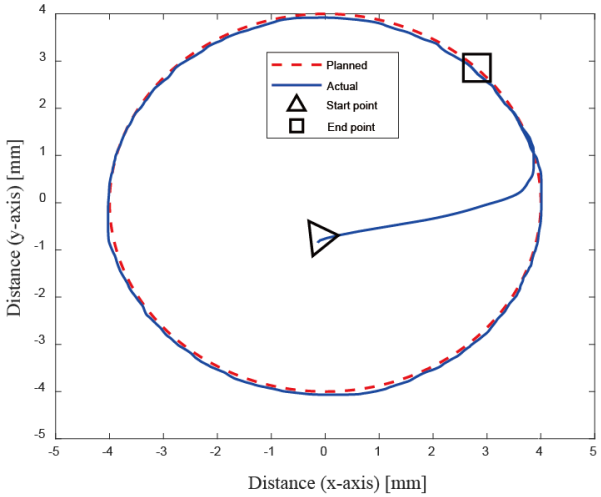

Figure 12. The tracking response of the circular trajectory.

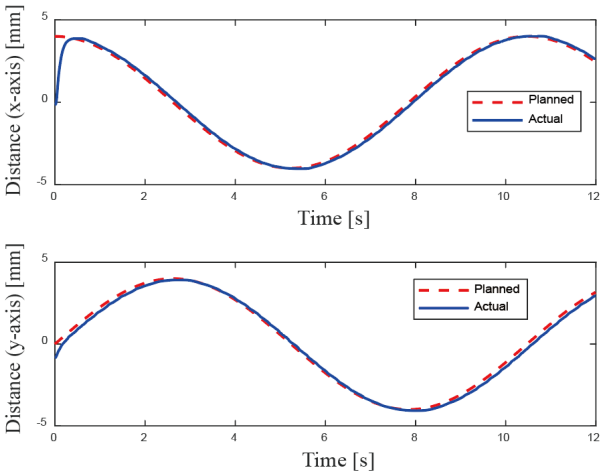

Figure 13. Response of the circular trajectory tracking in x and y-axes.

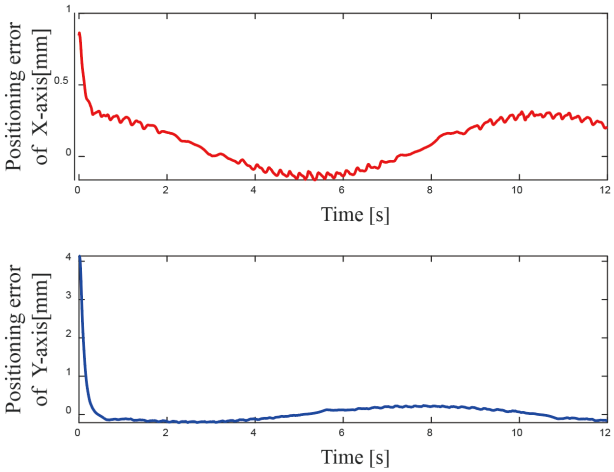

Figure 14. Responses of the circular trajectory tracking errors in x and y-axes.

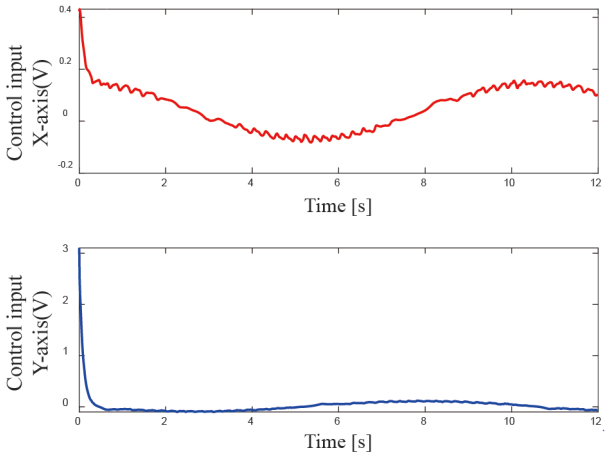

Figure 15. The control signal based on decentralized PID with circular trajectory.

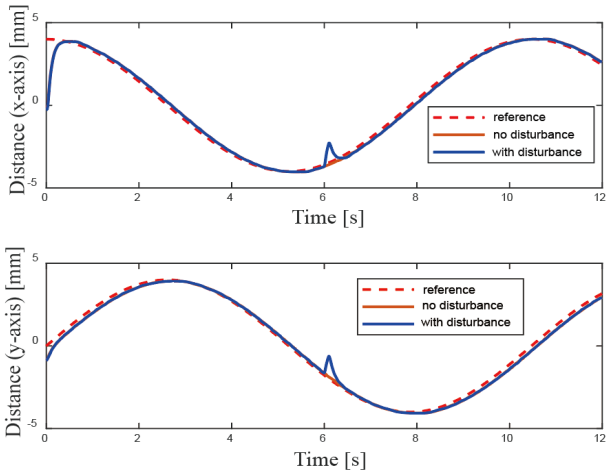

Figure 16. Response of the circular trajectory tracking with a sudden disturbance in x and y-axes.

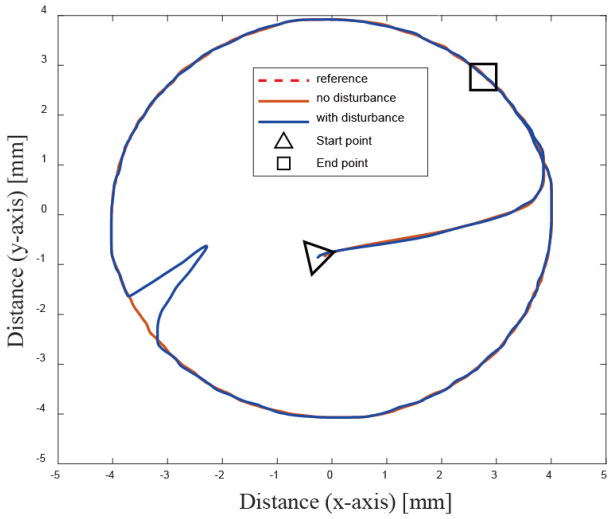

Figure 17. Tracking response of the circular trajectory with a sudden disturbance

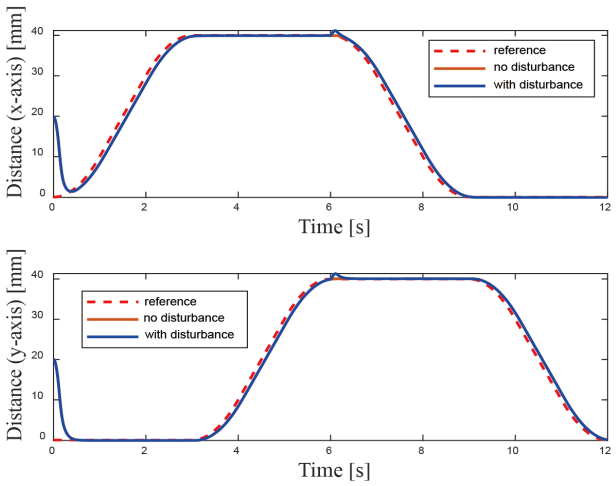

Figure 18. Response of the square trajectory tracking with a sudden disturbance in x and y-axes.

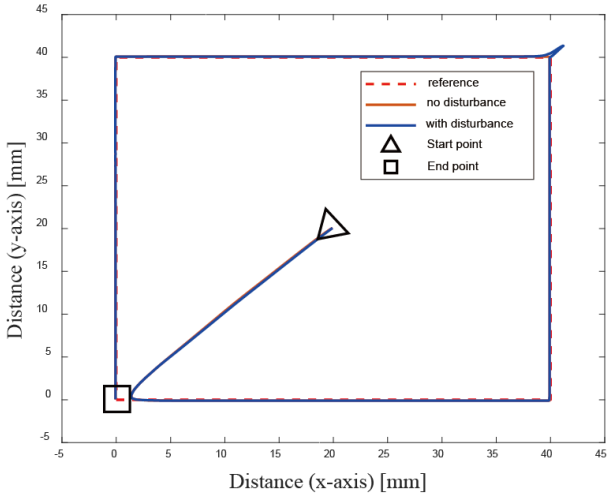

Figure 19. Tracking response of the circular trajectory with a sudden disturbance.

Conclusion

In this study, the motion trajectories with a trapezoidal velocity profile and circular interpolation profile are planned and applied to the X-Y platform. Then, decentralized PID controllers are designed to achieve the precise positioning control. The experimental results display the satisfactory performance with the maximum tracking error 0.02265 mm in the square trajectory and 0.0164 mm in the circular trajectory. Furthermore, motion process satisfies the planned T-curve velocity and circular interpolation profile such that the controlled system possesses the smoother movement in the presence of input saturations or a sudden disturbance. Directly, the experiments validate the effectiveness and feasibility of the proposed control scheme.

REFERENCES

Biagiotti, L., and Melchiorri, C., "Optimization of generalized S-curve trajectories for residual vibration suppression and compliance with kinematic bounds," IEEE/ASME Transactions on Mechatronics, Vol. 26, No. 5, pp. 2724-2734 (2021).

Chang, C. C., Hsia, S. Y., and Huang, H. D., "Improvement on CNC drilling quality using vibration suppression fixture," IEEE International Conference on Applied System Invention (2018).

Guo, L., Chen, H., Liu, Q., & Gao, B., "A computationally efficient and hierarchical control strategy for velocity optimization of on-road vehicles," IEEE Transactions on Systems, Man, and Cybernetics: Systems, Vol. 49, No. 1, pp. 31-41 (2019).

Heo, H. J., Son, Y., and Kim, J. M., "A trapezoidal velocity profile generator for position control using a feedback strategy," Energies, Vol. 12, No. 7, pp. 315-320 (2019).

Huang, X., Wang, Z., Zhang, Y., & Tan, Q., "Temperature rise calculation and velocity planning of permanent magnet linear synchronous motor under trapezoidal speed," CES Transactions on Electrical Machines and Systems, Vol. 6, No. 3, pp. 225–234 (2022).

Jindal, A., and Ragavan, K., "Sensorless control of switched reluctance motor based on trapezoidal inductance profile," Proceedings of the International Conference on Power Electronics, Drives and Energy Systems (2018).

Krikelis, N. J., and Barkas, S. K., "Design of tracking systems subject to actuator saturation and integrator wind-up," International Journal of Control, Vol. 39, No. 4, pp. 667-682 (1984).

Kung, Y. S., and Jou, S. H., "FPGA-Realization of Adaptive Fuzzy Controller for the Linear XY Table," Eighth International Conference on Intelligent Systems Design and Applications (2008).

Lan, H., Wang, W., Shangguan, Y., and Lin, S., "Fundamental studies on high power fiber laser cutting performance of 30 mm thick carbon steel plate," 6th International Forum on Strategic Technology (2011).

Liu, X., Wang, C., Xin, R., Li, M., and Tian, C., "A gain robust tuning method for PID controller based on vector model," Chinese Automation Congress (2015).

Masoudi, S., Feyzi, M. R., and Banna Sharifian, M. B., "Force ripple and jerk minimisation in double sided linear switched reluctance motor used in elevator application," IET Electric Power Applications, Vol. 10, No. 6, pp. 508-516 (2016).

Masuda, S., "Data-driven PID gain tuning for liquid level control of a single tank based on disturbance attenuation fictitious reference iterative tuning," 15th International Conference on Control Automation and Systems (2015).

Nguyen, D. T., Saussie, D., and Saydy, L., "Design and experimental validation of robust self-scheduled fault-tolerant control laws for a multicopter UAV," IEEE/ASME Transactions on Mechatronics, Vol. 26, No. 5, pp. 2548-2557 (2021).

Ohishi, K., and Mashimo, T., "Digital robust speed servo system with complete avoidance of output saturation effect," Proceedings of Power Conversion Conference (1997).

Ohishi, K., Hayasaka, E., Nagano, T., Harakawa, M., and Kanmachi, T., "High-performance speed servo system considering voltage saturation of a vector-controlled induction motor," IEEE Transactions on Industrial Electronics, Vol. 53, No. 3, pp. 795-802 (2006).

Tan, K. K., Li, X., Chen, S. L., Teo, C. S., and Lee, T. H., "Disturbance compensation by reference profile alteration with application to tray indexing," IEEE Transactions on Industrial Electronics, Vol. 66, No. 12, pp. 9406-9416 (2019).

Wang, S. Q., He, C. L., and Cao, Z. M., "Machining distortion in the milling of multi-frame components," Journal of Manufacturing Processes, Vol. 68 (2021).

Wang, X., Jiang, X., Chen, L., and Wu, Y., "A trajectory prediction method based on a variable-order Markov model with kernel smoothing," IEEE Access, Vol. 6, pp. 25200-25208 (2018).

Wu, J., Song, H., Wan, L., Abbass, K., and Hassan, T., "Robust Design for Multiple Quality Characteristics of Precision Product Using Taguchi-based Hybrid Method," IEEE International Conference on Industrial Engineering and Applications (2022).

Yoon, H. J., Chung, S. Y., Kang, H. S., & Hwang, M. J., "Trapezoidal motion profile to suppress residual vibration of flexible object moved by robot," Electronics, Vol. 8, No. 1 (2019).